

Synthesis, Characterization, and Properties of High Molecular Weight Poly(methylated ferrocenylsilanes) and Their Charge Transfer Polymer Salts with Tetracyanoethylene

John K. Pudelski, Daniel A. Foucher, Charles H. Honeyman, Peter M. Macdonald, and Ian Manners*

Department of Chemistry, University of Toronto, 80 St. George Street, Toronto, Ontario M5S 1A1, Canada

Stephen Barlow and Dermot O'Hare*

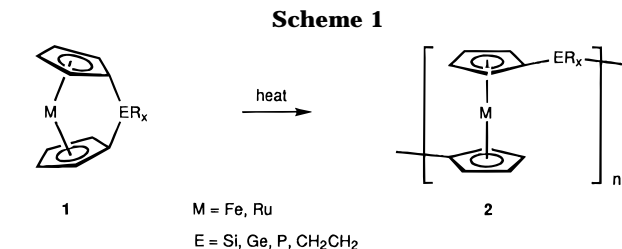
Inorganic Chemistry Laboratory, University of Oxford, South Parks Road, Oxford, OX1 3QR, U.K.

Received August 14, 1995; Revised Manuscript Received November 14, 1995[®]

ABSTRACT: A series of poly(ferrocenylsilanes) with methylated cyclopentadienyl (Cp) rings $[\text{Fe}(\eta\text{-C}_5\text{-Me}_x\text{H}_{4-x})(\eta\text{-C}_5\text{Me}_y\text{H}_{4-y})\text{SiMe}_2]_n$ (**2a–e**) (**a**, $x = 0$, $y = 0$; **b**, $x = 1$, $y = 1$ (Cp–Me groups at random positions); **c**, $x = 1$, $y = 1$ (Cp–Me groups at 3,3' positions); **d**, $x = 4$, $y = 0$; **e**, $x = 4$, $y = 4$) have been prepared by thermal ring-opening polymerization (TROP) of the corresponding silicon-bridged [1]ferrocenophanes $\text{Fe}(\eta\text{-C}_5\text{Me}_x\text{H}_{4-x})(\eta\text{-C}_5\text{Me}_y\text{H}_{4-y})\text{SiMe}_2$ (**1a–e**). DSC analysis revealed that increasing methylation of the ferrocenophane Cp rings resulted in increasing onset temperatures for the TROP reaction but did not significantly affect the enthalpy of polymerization, ΔH_p . Poly(ferrocenylsilanes) **2b–d** were soluble in common organic solvents and were characterized by IR, ^1H , ^{13}C , and ^{29}Si NMR spectroscopy, and elemental analysis. The molecular weights of these polymers were estimated to be in the range of $M_w = 1.8 \times 10^5$ to 4.1×10^5 and $M_n = 9.4 \times 10^4$ to 2.8×10^5 by GPC in THF versus polystyrene standards. The fully methylated poly(ferrocenylsilane) **2e** was insoluble in common organic solvents and was characterized by IR, ^{13}C and ^{29}Si CP-MAS NMR, and elemental analysis. The electrochemical behavior of **2b–d** in CH_2Cl_2 solution was investigated by cyclic voltammetry, and these polymers each exhibited two reversible oxidation waves, consistent with significant electronic interactions between the iron centers. Increasing Cp methylation led to the expected decrease in half-wave oxidation potentials, relative to nonmethylated **2a**. DSC analysis showed that **2b–d** exhibit weak glass transitions which shift to higher temperature with increasing methylation. No melting transitions were detected by DSC for these polymers, and WAXS analysis confirmed that the polymers were amorphous and indicated that the average interchain distance increases with increasing Cp methylation. TGA of **2a–d** found decreasing thermal stability with regard to weight loss upon increasing methylation. The microstructure of polymer **2d** provided insight into the polymerization mechanism and was consistent with polymerization via nonselective cleavage of Cp–Si (as opposed to Cp–Fe) bonds. The reactions of **2a**, **2b**, **2d**, and **2e** with tetracyanoethylene (TCNE) were investigated. Whereas **2a** did not react, the Cp-methylated analogues **2b**, **2d**, and **2e** yielded dark solids **3b**, **3d**, and **3e**, which were soluble in polar organic solvents. IR and microanalytical data indicated that the products contain oxidized polymer and a mixture of polycyano counteranions. Bulk solid-state magnetic susceptibility data indicated that **3e** obeys the Curie–Weiss law, with $\mu_{\text{eff}} = 2.0 \mu_B$, and $\theta = -1.1 \text{ K}$. In contrast to recent reports on TCNE-oxidized oligo(ferrocenylsilanes), no evidence was found for any long-range cooperative spin–spin interactions at low temperature.

Introduction

Metallocenes are attracting considerable attention as components of solid state and polymeric materials with novel physical properties.^{1–9} We have previously shown¹⁰ that thermal ring-opening polymerization (TROP) of silicon-bridged [1]ferrocenophanes (**1**, $M = \text{Fe}$, $\text{ER}_x = \text{SiR}_2$) provides access to high molecular weight ($M_w = 10^5$ – 10^6) poly(ferrocenylsilanes) (**2**, $M = \text{Fe}$, $\text{ER}_x = \text{SiR}_2$), a class of polymers which had been previously prepared in low molecular weight form ($M_w < 7000$) by condensation routes.¹¹ Recently, we have found that ring-opening polymerization of silicon-bridged [1]ferrocenophanes can also be achieved in solution at room temperature in the presence of anionic initiators or transition metal catalysts.^{12–14} The ring-opening polymerization methodology has been found to be quite general for strained metallocenophanes, and we have reported the successful preparation of a variety of organometallic polymers by TROP, such as poly(ferrocenylgermanes) (**2**, $M = \text{Fe}$, $E = \text{Ge}$),¹⁵ poly(ferro-

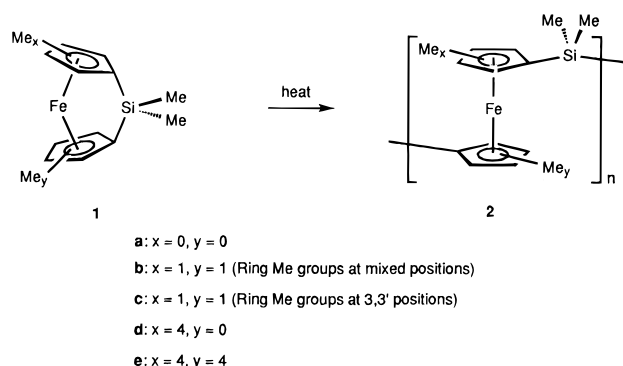


cenylphosphines) (**2**, $M = \text{Fe}$, $E = \text{P}$),⁸ and poly(ferrocenylethylenes) (**2**: $M = \text{Fe}$, $\text{ER}_x = \text{CH}_2\text{CH}_2$)¹⁶ and poly(ruthenocenylethylenes) (**2**, $M = \text{Ru}$, $\text{ER}_x = \text{CH}_2\text{CH}_2$).¹⁷ As expected, the properties of these materials have been found to vary substantially and depend on the nature of the metal M and the bridging moiety, ER_x present.⁸

The physical characteristics of poly(ferrocenylsilanes) have been found to depend significantly on the side groups attached to silicon.^{8,18–20} For example, whereas **2** ($M = \text{Fe}$, $\text{ER}_x = \text{SiMe}_2$) is a crystallizable thermoplastic with a glass transition (T_g) above room temperature, the *n*-hexyl analog **2** ($M = \text{Fe}$, $\text{ER}_x = \text{Si}^i\text{Hex}_2$) is an

[®] Abstract published in *Advance ACS Abstracts*, January 15, 1996.

Scheme 2



amorphous gum with a T_g of -26°C . Substitution of the Cp ring offers an alternative opportunity to control the properties of poly(ferrocenylsilanes). Previous work has shown that methylation of the Cp rings is a well-established method for modifying the optical, electronic, magnetic, and catalytic properties of metallocene-based molecules and materials.^{21–25} For example, oxidation of molecular metallocene species with methylated Cp rings (e.g., $M(\eta\text{-C}_5\text{Me}_5)_2$; $M = \text{Fe, Cr, Mn}$) with reagents such as TCNE and TCNQ has afforded materials which exhibit low-temperature ferromagnetic behavior.^{2,26} With this in mind, oxidation of poly(ferrocenylsilanes) with methylated Cp rings represents a potentially attractive route to materials with interesting magnetic properties. Indeed, Garnier and co-workers recently reported^{20d} the low-temperature ferromagnetic behavior of TCNE-oxidized oligo(ferrocenylsilanes) ($M_w = \text{ca. } 1500$). Methylation of the Cp rings also offers control of poly(ferrocenylsilane) morphology and thermal transition behavior as Cp methylation can clearly be expected to increase the bulkiness and rigidity of the ferrocenyl moiety present in the repeat units.

With these considerations in mind, we recently described the synthesis and structures of a series of strained, silicon-bridged [1]ferrocenophanes with methylated Cp rings.²⁷ In this paper, we report in detail our studies of the TROP reactions of these methylated ferrocenophanes and the characterization and properties of the resulting series of poly(ferrocenylsilanes) with methylated Cp rings and their TCNE-oxidized products.

Results and Discussion

1. TROP of the Ferrocenophanes with Methylated Cyclopentadienyl Rings. When heated in the melt, methylated silicon-bridged [1]ferrocenophanes **1b–e** underwent TROP to afford the corresponding poly(ferrocenylsilanes) with methylated Cp rings (Scheme 2). Prior to bulk-scale reactions, the TROP reactions were followed by differential scanning calorimetry (DSC) to determine optimal thermal reaction conditions. Bulk TROP reactions of **1b–d** afforded soluble, high molecular weight polymeric products which could be fully characterized. In contrast, bulk TROP reactions of **1e** afforded an insoluble product which was characterized by solid-state NMR and elemental analysis.

(a) DSC Studies of the TROP Reactions of the Methylated Ferrocenophanes. We have previously described the use of DSC to monitor the TROP reactions of strained silicon-bridged [1]ferrocenophanes.¹⁰ The DSC heating scans of these species show sharp melt endotherms followed by large, broad exotherms at higher temperatures which are assigned to the TROP reaction. The cooling scans generally show no transitions, indicating complete TROP reaction under the

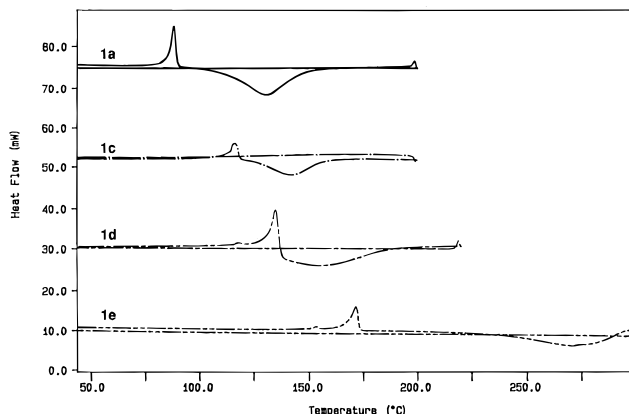


Figure 1. DSC thermograms of the TROP reactions of silicon-bridged [1]ferrocenophanes **1a**, **1c**, **1d**, and **1e**.

Table 1. Melting Onsets, TROP Onsets, and TROP Exotherm Areas for Silicon-Bridged [1]Ferrocenophanes **1a–e^a**

ferrocenophane	mp (°C)	TROP onset (°C)	TROP exotherm area (kJ·mol ⁻¹) ^b
1a	90	107	80 ^c
1b	^d	123	73
1c	113	122	73
1d	131	137	72
1e	167	238	81

^a Obtained by DSC analysis at $10^\circ\text{C}\cdot\text{min}^{-1}$ under N_2 . ^b Represent an average of three independent analyses and are reported $\pm 5 \text{ kJ}\cdot\text{mol}^{-1}$. ^c Taken from ref 10. ^d This mixture of isomers is obtained as a viscous liquid and does not exhibit a melting point.

conditions of the DSC experiment. Our DSC experiments, typically run on a 5 mg scale, provide a valuable and economical method of estimating the temperature at which TROP of a particular monomer occurs. This information can then be exploited in carrying out bulk polymerization reactions. DSC analysis is also useful in probing the effect of structural modifications of the monomer on polymerization reactivity. Figure 1 shows an overlay of the DSC traces obtained by analysis of the TROP reactions of **1a** and **1c–e** at a heating rate of $10^\circ\text{C}\cdot\text{min}^{-1}$ under N_2 . Each DSC trace shows a sharp melt endotherm followed by a large, broad polymerization exotherm on the forward (heating) scan, consistent with the ferrocenophanes undergoing TROP after entering the melt. The DSC trace of the TROP reaction of **1b** exhibited a large TROP exotherm but no melt endotherm since this material, consisting of a mixture of isomers, is obtained as a viscous liquid. Table 1 summarizes melting and TROP onset temperatures for the ferrocenophanes **1a–e**. Return (cooling) scans show no transitions, indicating that the TROP reactions are complete under the conditions of the DSC experiment. After DSC analysis, samples were analyzed by ^1H NMR and GPC, which, in the case of **1a–d**, confirmed complete conversion of the ferrocenophane to poly(ferrocenylsilane) high polymer. The DSC reaction of **1e** afforded an insoluble product which could not be analyzed by ^1H NMR or GPC.

The DSC traces clearly indicate that each of the crystalline ferrocenophanes enters the melt prior to TROP. For **1c** and **1d**, the TROP exotherm immediately follows the melt endotherm. For **1a**, a brief temperature delay between melt and TROP was observed, and for **1e**, a more substantial delay between melt and TROP was detected. Notably, the 3,3'-syn isomer **1c** and the mixed isomer analog **1b** exhibit essentially the same TROP onset temperature despite the fact that the

former compound is crystalline and exhibits a melt prior to TROP and the latter is a viscous liquid at room temperature. These findings suggest that ferrocenophane melting is necessary but not sufficient for TROP.

An intriguing finding from the DSC study is the increase in TROP onset temperature which is observed with increasing methylation of the Cp rings. Particularly striking is the high onset temperature (ca. 240 °C) observed for TROP of fully methylated **1e**. One possible explanation for this trend in onset temperatures is that TROP depends only on the ferrocenophane entering the melt. Thus, increases in the TROP onset temperatures result from increases in the ferrocenophane melting points which are observed with increasing methylation. However, the findings described above suggest that melting is necessary but not sufficient for TROP. An alternative explanation for the increases in TROP onset with increasing ferrocenophane methylation involves electronic or steric effects of the Cp methyl substituents. Steric effects would be expected to be important since Cp methyl group steric shielding of the bridging silicon atom and/or steric deactivation of any propagating species would clearly hinder TROP. Electron donating Cp methyl substituents would also be expected to hinder any polymerization pathway which involved a buildup of negative charge on the Cp rings.²⁸

While Cp methylation resulted in a pronounced increase of the TROP onset temperature, it did not have a substantial effect on the ΔH of the TROP reaction (ΔH_p). Table 1 summarizes TROP exotherm areas for **1a–e**, obtained by integration of the TROP exotherms in the DSC traces, which provide a measure of ΔH_p . TROP exotherm areas of similar magnitude were observed for all of the methylated ferrocenophanes **1b–e**, and these values are similar to that previously observed for nonmethylated **1a** (ca. 80 kJ·mol⁻¹).¹⁰

(b) Preparative TROP Reactions of the Methylated Ferrocenophanes: Characterization of the Poly(ferrocenylsilanes) with Methylated Cyclopentadienyl Rings. (i) **TROP of 1b and 1c.** Based on the findings of the DSC study, preparative-scale TROP reactions of the methylated ferrocenophanes were carried out. A sample of **1c** was sealed under vacuum in a Pyrex tube and heated at 150 °C. The sample melted, the melt increased rapidly in viscosity, and after ca. 15 min, the sample was immobile. The tube was cooled and cracked open, and poly(ferrocenylsilane) **2c** was obtained as an orange fibrous solid in 91% yield by dissolution of the crude polymerization mixture in THF followed by precipitation into methanol. The material was found to be highly soluble in common organic solvents (e.g., THF, C₆H₆, and CH₂Cl₂), and GPC analysis indicated that it was monomodal and of high molecular weight ($M_w = 1.8 \times 10^5$, $M_n = 9.4 \times 10^4$). Poly(ferrocenylsilane) **2b** was obtained from TROP of **1b** under identical conditions in 53% yield, also as an orange fibrous solid soluble in common organic solvents. GPC analysis of **2b** found it to be monomodal and of high molecular weight ($M_w = 4.1 \times 10^5$, $M_n = 2.8 \times 10^5$).

NMR analysis of poly(ferrocenylsilanes) **2b** and **2c** clearly demonstrated the differences in materials which are obtained from TROP of a single dimethylated ferrocenophane isomer and from TROP of a mixture of dimethylated ferrocenophane isomers. Figure 2 shows the ¹H NMR spectra of **2b** and **2c**. The ¹H NMR spectrum of **2b** consists of three broad, overlapping bands in the Cp region (4.32–3.66 ppm), a broad structured band in the Cp–Me region (1.93–1.78 ppm), and a single broad band in the Si–Me region (0.78–0.49 ppm). The broadness of the resonances reflects the

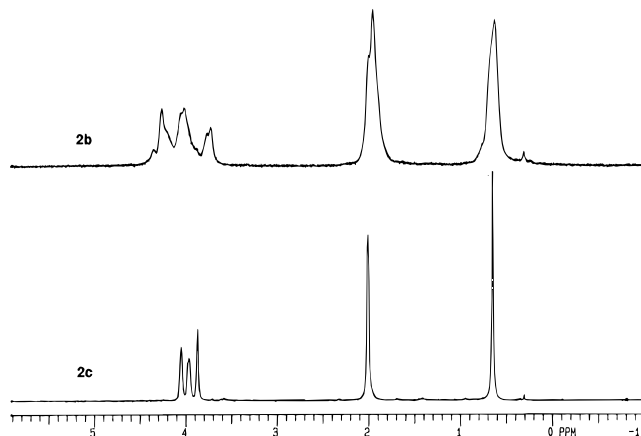


Figure 2. 200 MHz ¹H NMR spectra of **2b** and **2c** in C₆D₆.

multiple environments of Cp, Cp–Me, and Si–Me protons in the isomeric ferrocenyl repeat units. Conversely, the ¹H NMR spectrum of **2c** shows sharp resonances for the Cp (4.03, 3.95, 3.86 ppm), Cp–Me (2.00 ppm), and Si–Me (0.63 ppm) protons in the isomerically equivalent repeat units. Similar differences were observed in the ¹³C and ²⁹Si NMR spectra of **2b** and **2c**.

(ii) TROP of 1d: Mechanistic Implications of the Microstructure of 2d. The TROP reaction of unsymmetrically methylated **1d** provides information regarding the mechanism of the TROP reaction of silicon-bridged [1]ferrocenophanes.²⁸ Although there has been considerable progress concerning the scope of the TROP route and the properties of the resulting polymeric materials, to date, nothing has been reported regarding the mechanism of the polymerization reactions. In particular, the fundamental question of whether the TROP reactions proceed via cleavage of bonds between *ipso* Cp carbon atoms and bridging atoms or, alternatively, via cleavage of metal–Cp bonds remains unresolved. A report that reaction of ferrocene and 1,1'-dimethylferrocene at 250 °C affords a 60% yield of methylferrocene suggests that an Fe–Cp cleavage mechanism for TROP of silicon-bridged [1]ferrocenophanes cannot be ruled out, especially since Fe–Cp bonding (and Si–Cp also) is likely to be weakened in these strained species. Indeed, the Fe–Cp bond energy of ferrocene (220 kJ/mol) is considerably lower than the typical Si–C bond energy (318 kJ/mol).²⁹ Furthermore, we have recently observed facile, thermally induced M–(π-hydrocarbon) bond cleavage in reactions of related silicon-bridged metalloarenophanes. For example, the Cr–(η-C₆H₆) bond energy of Cr(η-C₆H₆)₂ is ca. 170 kJ/mol²⁹ and thermolysis of Cr(η-C₆H₅)₂SiMe₂ at 180 °C yields Cr metal and Ph₂SiMe₂ as the exclusive products.³⁰ Studies of the poly(ferrocenylsilane) product resulting from TROP of **1d** have allowed us to distinguish between a Si–Cp bond cleavage and an Fe–Cp bond cleavage mechanism of polymerization.

We reasoned (Figure 3) that if TROP of **1d** proceeded through Si–Cp^H and Si–Cp^{Me} bond cleavage (Cp^H = η-C₅H₄, Cp^{Me} = η-C₅Me₄), then the resulting polymeric product **2d** would contain three silicon environments (Cp^HSiCp^H, Cp^{Me}SiCp^H, and Cp^{Me}SiCp^{Me}) but only a single iron environment (Cp^HFeCp^{Me}). Conversely, if Fe–Cp^H and Fe–Cp^{Me} cleavage occurred, then polymeric product **2d'** would contain a single silicon environment (Cp^HSiCp^{Me}) but three iron environments (Cp^HFeCp^H, Cp^{Me}FeCp^H, and Cp^{Me}FeCp^{Me}). We felt that the two cleavage possibilities would be unambiguously distinguished by using ¹H, ¹³C, and ²⁹Si NMR to probe

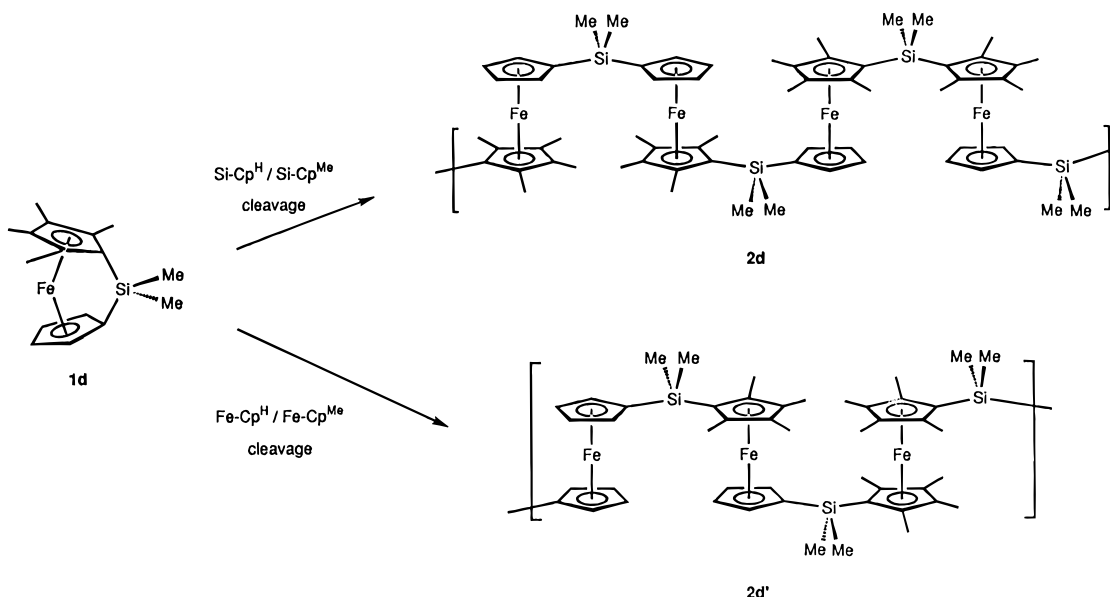


Figure 3. Bond cleavage possibilities in the TROP of silicon-bridged [1]ferrocenophane **1d**.

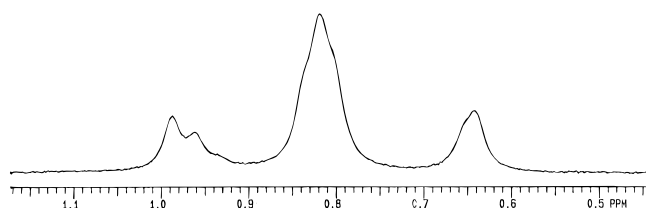


Figure 4. Expansion of the Si-Me region of the ^1H NMR spectrum (200 MHz, C_6D_6) of **2d**.

the silicon environments of the poly(ferrocenylsilane) product and by using cyclic voltammetry to probe the iron environments.

TROP of **1d** was effected by heating the compound in the melt at 150 °C in an evacuated, sealed Pyrex tube. The resulting orange, fibrous product, obtained in 63% yield, was completely soluble in THF and other common organic solvents and was purified by precipitation into methanol. GPC analysis found the material to be monomodal and of high molecular weight ($M_w = 3.4 \times 10^5$, $M_n = 2.3 \times 10^5$).

Analysis of the polymer microstructure by ^1H NMR led to the detection of three broad resonances in the SiMe_2 region in a 1:2:1 integral ratio centered at 0.98, 0.82, and 0.64 ppm, respectively (Figure 4). Similarly, ^{29}Si NMR analysis of polymer microstructure gave three sets of resonances, in an approximately 1:2:1 intensity ratio, centered at -4.05 , -6.42 , and -6.77 ppm, and ^{13}C NMR also showed three sets of resonances in the SiMe_2 region at 5.1, 1.5, and -0.22 to -0.26 ppm. These results clearly indicated the presence of three types of silicon environments in the polymer in a statistical ratio and therefore showed that TROP of **1d** proceeds via nonselective cleavage of Si-Cp^{H} and Si-Cp^{Me} bonds to afford poly(ferrocenylsilane) **2d** (Figure 3). Such lack of selectivity is not surprising for a high-temperature reaction which proceeds neat in the melt. As mentioned above, TROP of **1d** via exclusive cleavage of the Si-Cp^{H} and Si-Cp^{Me} bonds should afford a polymeric product in which all of the iron atoms exist in a $\text{Cp}^{\text{H}}\text{FeCp}^{\text{Me}}$ environment. Analysis of **2d** by cyclic voltammetry and also ESR data on the TCNE-oxidized product **3d** clearly confirmed this expectation (see below). The TROP of **1d** probably represents a good general model for the polymerization of other silicon-bridged [1]ferrocenophanes since the melt polymerizations occur under quite similar conditions.⁸

(iii) TROP of 1e. Based on the DSC findings, we heated a sample of fully methylated ferrocenophane **1e** at 265 °C to effect TROP. As expected, the monomer melted and then gradually became immobile, and a powdery orange solid was obtained in 65% yield. The only other material isolated from this reaction was unreacted **1e**. We were surprised, however, to find that the orange solid product is insoluble in all of the organic solvents which we have examined (e.g., C_6H_6 , CH_2Cl_2 , THF, DMSO, NMP, DMF).

The insoluble nature of the TROP product of **1e** precluded straightforward characterization via solution methods but ^{13}C and ^{29}Si CP-MAS NMR analysis provided data consistent with polymeric structure **2e**. A single sharp peak at -1.6 ppm was observed in the ^{29}Si CP-MAS spectrum. In the ^{13}C CP-MAS spectrum, two broad intense peaks at 82–85 ppm and a peak of low intensity at 69 ppm were observed in the Cp region and a single broad and intense peak was observed at 14–18 ppm. We assign the latter signal to the Cp methyl carbons and the silyl methyl carbons, which do not resolve. The peak of low intensity at 69 ppm is assigned to the *ipso* Cp carbons. The shift of the *ipso* carbon resonance from 25.6 ppm in the ^{13}C NMR spectrum of ferrocenophane **1e** to 69 ppm in the insoluble product is consistent with TROP reaction to yield **2e**. Unusually high field ^{13}C NMR chemical shifts (e.g., 20–30 ppm) are observed for the *ipso* Cp carbons of [1]ferrocenophanes and have been attributed to structural distortions arising at the *ipso* sites due to the tilted Cp rings.³¹ During TROP, these distortions are relieved as unstrained ferrocenyl repeat units with parallel Cp rings are generated and more typical *ipso* shifts (e.g., 68–72 ppm) are then observed for the resulting poly(ferrocenylsilanes). The peaks at 82–85 ppm are assigned to the remaining (α and β) Cp carbons of **2e**. These Cp peaks are shifted downfield relative to the shifts observed for analogous carbon atoms in the CP-MAS NMR spectrum of poly(ferrocenyldiphenylsilane).¹⁸ Downfield ^{13}C NMR shifts of Cp carbons upon methylation are observed in solution spectra for both the soluble methylated polymers (i.e., **2b–d** relative to **2a**) and the methylated monomers (i.e., **1b–e** relative to **1a**). Thus, the downfield shifts of the Cp carbon resonances in the CP-MAS spectrum of **2e**, relative to poly(ferrocenyldiphenylsilane), are consistent with a

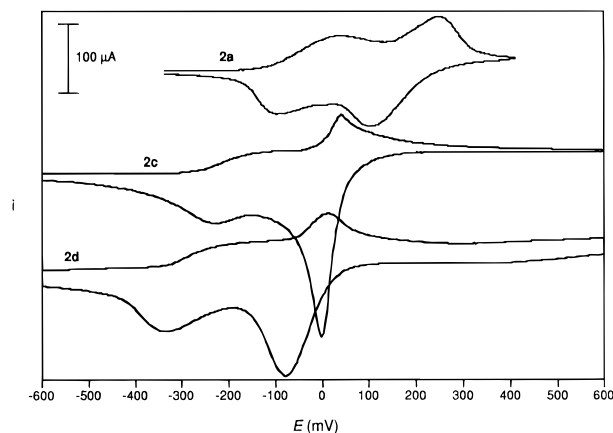


Figure 5. Cyclic voltammograms of CH_2Cl_2 solutions of **2a**, **2c**, and **2d** referenced to the ferrocene/ferrocenium ion couple at $E = 0.00$ V.

polymeric structure with fully methylated Cp rings. Elemental analysis of the TROP product of **1e** was also fully consistent with polymeric structure **2e**.

2. Electrochemical and Electronic Properties of Poly(ferrocenylsilanes) with Methylated Cyclopentadienyl Rings. We have studied the electrochemical and electronic properties of the poly(ferrocenylsilanes) with methylated Cp rings using cyclic voltammetry and UV-vis spectroscopy, respectively. Because of the observed insolubility, fully methylated **2e** was not included in these studies.

(a) Cyclic Voltammetry of Poly(ferrocenylsilanes) 2b–d. Previous studies of poly(ferrocenylsilanes) have shown that, in solution, these materials yield cyclic voltammograms (CVs) consisting of two reversible waves of approximately equal intensity.^{8,10} We have attributed this response to the oxidation of alternating iron centers along the polymer backbone at the first wave ($E = {}^1E_{1/2}$) followed by oxidation of the iron centers in between at higher potential ($E = {}^2E_{1/2}$).¹⁰ The separation of the two waves, ΔE , provides a measure of the electronic interaction between the iron centers in the polymer backbone. Manipulation of the substituents at silicon leads to modest changes in poly(ferrocenylsilane) $E_{1/2}$ and ΔE values, most likely due to weak side group electronic effects and/or polymer conformational effects which result from side group manipulation.⁸ We anticipated that methylation of the Cp rings of poly(ferrocenylsilanes) would have a much more dramatic effect on the cyclic voltammetric response of these materials than manipulation of the side groups at silicon. The effect of Cp methylation on the electronic properties of molecular ferrocene species has been studied by a variety of techniques including cyclic voltammetry. For example, Gassman has shown that the cyclic voltammetric oxidation potentials of methylated ferrocene derivatives are reduced by ca. 55 mV, relative to ferrocene, per electron-donating methyl substituent.²² Figure 5 shows an overlay of CVs obtained from analysis of CH_2Cl_2 solutions of **2a**, **2c**, and **2d**, and Table 2 lists ${}^1E_{1/2}$, ${}^2E_{1/2}$, and ΔE data for these polymers. The CV of **2b** was nearly identical to that of **2c** and for simplicity is not shown in Figure 5. For each polymer, the expected two-wave response was observed. Linear plots of i_{peak} vs square root of scan rate indicate that both the first and second oxidation processes are diffusion controlled for each polymer over a 25–1000 $\text{mV}\cdot\text{s}^{-1}$ range of scan rates. With increasing Cp methylation, both the first and second oxidation waves for each polymer shifted to lower oxidation potentials as can be

Table 2. Cyclic Voltammetry Data for Poly(ferrocenylsilanes) 2a–d^a

polymer	${}^1E_{1/2}^b$	${}^2E_{1/2}^b$	ΔE (V) ^c
2a	−0.03	0.17	0.20
2b	−0.16	0.04	0.20
2c	−0.17	0.02	0.19
2d	−0.25	−0.03	0.22

^a Data obtained by analysis at 22 °C of CH_2Cl_2 solutions which were ca. 5×10^{-3} M in polymer and 0.1 M in $[\text{NBu}_4][\text{PF}_6]$ at a scan rate of 250 $\text{mV}\cdot\text{s}^{-1}$. ^b ${}^1E_{1/2}$ and ${}^2E_{1/2}$ are the half-wave oxidation potentials for the first and second oxidation waves in the polymer CVs, respectively, and are given in volts vs the ferrocene/ferrocenium ion couple at $E = 0.00$ V by definition. ^c $\Delta E = {}^2E_{1/2} - {}^1E_{1/2}$.

seen from Figure 5. Inspection of the data in Table 2 reveals that, for the methylated polymers, both ${}^1E_{1/2}$ and ${}^2E_{1/2}$ are reduced by approximately the expected 55 mV per Cp methyl substituent relative to nonmethylated **2a**. The polymer ΔE values are similar, indicating that Cp methylation does not dramatically influence the interaction among the iron centers in the polymer backbone.

As discussed above, cyclic voltammetric analysis of **2d** clearly confirmed the presence of Fe atoms in a single type of electronic environment and thus confirmed that TROP of **1d** proceeds via cleavage of $\text{Si}-\text{Cp}^{\text{H}}$ and $\text{Si}-\text{Cp}^{\text{Me}}$ bonds. The CV of **2d** showed the expected two oxidation waves of equal intensity ($E_{1/2} = -0.25$ and -0.03 V) with shapes that were modified by electrode adsorption effects (Figure 5). This two-wave response is completely analogous to that of the other poly(ferrocenylsilanes) and is consistent with initial oxidation at alternating iron sites along the polymer backbone followed by subsequent oxidation, at a higher potential, of the iron centers in between. Thus, the CV confirms the presence of only a single type of iron environment in **2d**. Moreover, the $E_{1/2}$ value (-0.25 V vs ferrocene/ferrocenium; -0.22 V vs **2a**) observed for the first oxidation wave is consistent with the presence of iron atoms in a $\text{Cp}^{\text{H}}\text{FeCp}^{\text{Me}}$ environment which would be expected from TROP of **1d** via cleavage of $\text{Si}-\text{Cp}^{\text{H}}$ and $\text{Si}-\text{Cp}^{\text{Me}}$ bonds.

(b) UV-vis Studies of Poly(ferrocenylsilanes) 2b–d. The UV-vis spectroscopy of ferrocene and its derivatives has been studied extensively.³² Briefly, five bands are observed in the spectra of ferrocene and its derivatives. Of these, the band II system (at 440 nm in ferrocene) has received considerable attention. Assigned to spin-allowed d–d transitions, this band system is convenient for study because it is reasonably intense and well-resolved from other bands in the spectra. Our UV-vis studies of poly(ferrocenylsilanes) **2a–d** focused exclusively on the band II system.

Table 3 gives UV-vis band II data for a series of methylated ferrocene derivatives, silicon-bridged [1]-ferrocenophane monomers **1a–e**, and poly(ferrocenylsilanes) **2a–d**. Inspection of the data for the bridged and nonbridged molecular species reveals that increasing methylation leads to a blue shift of band II. Unexpectedly, we found that the absorption trend is reversed in the polymer series. Increasing methylation results in a red shift of band II.

3. Thermal Analysis and Morphology Studies of Poly(ferrocenylsilanes) with Methylated Cyclopentadienyl Rings. Our previous DSC studies of poly(ferrocenylsilanes) with nonmethylated Cp rings have shown that these materials exhibit weak glass transitions (T_g s) over a wide temperature range with the side groups at silicon exerting a considerable influence on

Table 3. UV-vis Data for Poly(ferrocenylsilanes) 2a-d and Small-Molecule Model Compounds^a

compound	λ_{\max} band II (nm)	ϵ band II ($\text{L}\cdot\text{mol}^{-1}\cdot\text{cm}^{-1}$) ($\times 10^{-2}$)
$\text{Fe}(\eta\text{-C}_5\text{H}_5)_2$	440	1.0
$\text{Fe}(\eta\text{-C}_5\text{H}_4\text{Me})_2$	438	1.6
$\text{Fe}(\eta\text{-C}_5\text{H}_5)(\eta\text{-C}_5\text{Me}_5)^b$	430	1.2
$\text{Fe}(\eta\text{-C}_5\text{HMe}_4)_2$	430	1.6
$\text{Fe}(\eta\text{-C}_5\text{Me}_5)_2^c$	420	1.2
1a	482	3.8
1b	481	3.7
1c	476	3.7
1d	473	3.4
1e	464	2.3
2a	442	2.3
2b	447	2.5
2c	460	2.3
2d	468	2.9

^a Data obtained by analysis of THF solution unless otherwise noted. Poly(ferrocenylsilane) **2e** is insoluble in THF and was not analyzed. ^b Data obtained by analysis of an isooctane solution. See: Chao, S.; Robbins, J. L.; Wrighton, M. S. *J. Am. Chem. Soc.* **1983**, *105*, 181. ^c Data obtained by analysis of a cyclohexane solution. See: King, R. B.; Bisnette, M. B. *J. Organomet. Chem.* **1967**, *8*, 287.

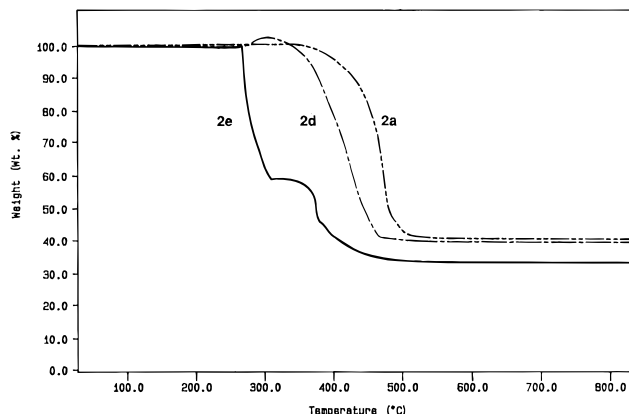
Table 4. Thermal Analysis Data for Poly(ferrocenylsilanes) 2a-e

polymer	T_g ($^{\circ}\text{C}$) ^a	T_{10} ($^{\circ}\text{C}$) ^{b,c}	T_{50} ($^{\circ}\text{C}$) ^{b,c}
2a	33 ^d	431	518
2b	93	404	471
2c	73	392	457
2d	116	382	445
2e		273	366

^a Obtained by DSC analysis at $10^{\circ}\text{C}\cdot\text{min}^{-1}$ under N_2 . ^b Obtained by TGA at $10^{\circ}\text{C}\cdot\text{min}^{-1}$ under N_2 . ^c T_{10} and T_{50} correspond to the temperatures at which the polymer sample has lost 10% and 50%, respectively, of its initial mass and represent an average of at least three independent analyses. ^d Taken from ref 18.

the T_g .⁸ For example, as the *n*-alkyl substituents at silicon increase in length from Me to *n*-Hex, poly(ferrocenylsilane) T_g decreases smoothly from $+33^{\circ}\text{C}$ to -26°C . Unsymmetrical poly(ferrocenylsilanes) are usually amorphous and generally do not exhibit melting transitions. In contrast, many of the symmetrically substituted analogues show a propensity to crystallize.^{8,33} We have also studied the thermal stability of poly(ferrocenylsilanes) by thermogravimetric analysis (TGA). Our TGA studies have found that, in general, poly(ferrocenylsilanes) are stable to weight loss through ca. 350°C at a heating rate of $10^{\circ}\text{C}/\text{min}$, at which point they suffer weight loss through ca. 800°C , ultimately affording thermally stable Fe/Si/C ceramic materials in yields ranging from 20 to 63% at 1000°C .³⁴ Stability to weight loss has been found to vary considerably as a function of the side groups at Si. We now describe the use of DSC and TGA to probe the effect of Cp methylation on poly(ferrocenylsilane) thermal transition behavior and stability to weight loss.

(a) DSC Analysis of Poly(ferrocenylsilanes) 2b-e. DSC analysis of the poly(ferrocenylsilanes) with methylated Cp rings revealed glass transitions with small heat capacity changes for **2b-d**. This behavior is consistent with the behavior of nonmethylated analogs. No T_g was observed for fully methylated **2e**. Table 4 lists T_g data for **2a-d**. Melting transitions were not observed during DSC analyses of **2b-e**, even after annealing at temperatures slightly above the observed T_g (100°C for **2e**) for 24 h. The data in Table 4 reveal an interesting trend in T_g among **2a-d**. Increasing methylation of the Cp rings leads to a smooth increase

**Figure 6.** TGA traces of poly(ferrocenylsilanes) **2e**, **2d**, and **2a**.

in polymer T_g . Cp methylation can readily be envisioned as increasing the steric bulk and rigidity of the ferrocenyl moieties of the polymer repeat units. Consistent with free volume interpretations of glass transition behavior, the increased rigidity and bulk of the repeat unit leads to increased polymer T_g . A similar increase in poly(ferrocenylsilane) T_g with increasing bulk and rigidity of the substituents at silicon has also been observed.^{8,19a} A second interesting finding was the slightly higher T_g observed for **2b** with mixed ring isomer repeat units relative to **2c** with a single isomeric repeat unit. This might be attributed to the presence of some methyl groups α to the main-chain Cp-Si bonds in the former material, which would be expected to lower the skeletal flexibility.

The morphology of methylated poly(ferrocenylsilanes) **2b-e** was also studied by wide-angle X-ray scattering (WAXS) at 25°C , and the scattering patterns of the methylated polymers were compared to the pattern of nonmethylated **2a**. The WAXS patterns of **2b-e** each consisted of a broad peak superimposed on amorphous halos, similar to the pattern for amorphous samples of **2a**.¹⁸ This behavior suggests the presence of only short-range order among these materials. Interestingly, d spacings corresponding to the broad peak in the polymer WAXS patterns increase with increasing Cp methylation. Thus, d spacings of 6.5, 6.9, 7.2, and 7.7 \AA were observed for **2a**, **2c**, **2d**, and **2e**, respectively. The d spacing of 6.37 \AA observed for **2a** has been assigned to interchain distances.³³ The increase in d spacing observed with increasing Cp methylation among **2a-e** is completely consistent with this assignment since Cp methylation would increase the steric bulk of the polymer backbone, thereby pushing the chains further apart, leading to increased interchain Fe-Fe distances.

(b) Thermogravimetric Analysis (TGA) of Poly(ferrocenylsilanes) with Methylated Cyclopentadienyl Rings. Thermogravimetric analysis of the methylated poly(ferrocenylsilanes) revealed that increasing Cp methylation leads to decreasing thermal stability toward weight loss. Figure 6 shows an overlay of TGA traces obtained from analysis of **2a**, **2d**, and **2e** at a heating rate of $10^{\circ}\text{C}\cdot\text{min}^{-1}$ under N_2 . For clarity, the TGA traces of **2b** and **2c** are not shown. Table 4 summarizes T_{10} and T_{50} data obtained from analysis of the TGA traces. It is obvious from the TGA studies that nonmethylated **2a** is the most stable to weight loss, fully methylated **2e** is the least stable, and thermal stability decreases smoothly with increasing Cp methylation. The most striking feature of these traces is the rapid weight loss suffered by **2e** beginning at ca. 280°C . This weight loss behavior proved to be completely reproducible and,

interestingly, corresponds to a mass loss equivalent to eight methyl groups. Again, differences are observed between **2b** with isomeric dimethylated repeat units and **2c** with isomerically equivalent dimethylated repeat units; as the former material was found to be slightly more stable to weight loss. These TGA studies suggest that thermal depolymerization of poly(ferrocenylsilanes) may be accelerated by methyl substitution of the cyclopentadienyl rings and/or that loss of Cp methyl substituents is an important poly(ferrocenylsilanes) thermal degradation pathway.

4. Reactions of Poly(ferrocenylsilanes) with TCNE. (a) **Reactions of Unmethylated Poly(ferrocenylsilanes) with TCNE.** Garnier et al. have recently reported studies on the magnetic properties of some oxidized ferrocene-based oligomers; specifically these workers reported that oligo(ferrocenylsilanes) undergo reactions with TCNE in dichloromethane yielding dark precipitates, which they formulated as $[\text{Fe}(\eta\text{-C}_5\text{H}_4)_2\text{SiR}_2]_n^{n+}[\text{TCNE}^-]_n$, which are ferromagnetic at low temperatures.^{20d} This reaction is quite surprising given that polymers of this type have redox potentials close to those of ferrocene.⁸ Ferrocene itself forms a complex with TCNE which is only dissociated to ionic species in polar solvents.^{35,36}

We investigated the reaction of the high molecular weight poly(ferrocenylsilanes) with TCNE to see if similar magnetically interesting products might be obtained. We added dichloromethane solutions of TCNE to dichloromethane solutions, or suspensions in the case of **2e**, containing equimolar quantities of polymer.

Neither the model linear trimetalocene $\text{Fe}(\eta\text{-C}_5\text{H}_4\text{-SiMe}_2\text{Fc})_2$ ($\text{Fc} = \text{Fe}(\eta\text{-C}_5\text{H}_4)(\eta\text{-C}_5\text{H}_5)$)¹² nor the high polymers **2a** and **2** ($\text{M} = \text{Fe}$, $\text{ER}_x = \text{SiBu}_2$) gave any visible reaction with TCNE; no precipitation or color changes were observed. IR spectroscopy of the residue remaining after solvent removal indicated the only cyano-carbon species present to be neutral TCNE,^{37–40} again indicating no reaction. This is what one would expect from the redox potentials of the materials, but is in contrast to the results found by Garnier et al. for materials apparently differing only in polymer chain length.

(b) **Reactions of Methylated Poly(ferrocenylsilanes) with TCNE.** Polymer **2e** is a much more attractive candidate for the formation of charge transfer materials: the permethylation of the Cp rings should lead to greater ease of oxidation. The expected charge transfer polymer salt would closely resemble $[\text{Fe}(\eta\text{-C}_5\text{-Me}_5)_2]^+[\text{TCNE}]^-$, which has been characterized as a molecular 3D ferromagnet. Addition of 1 equiv of TCNE to a suspension of **2e** in dichloromethane resulted in darkening of the mixture and dissolution of the polymer to yield a green-red dichroic solution with a small quantity of a brown insoluble residue. The major product, **3e**, was precipitated as a dark green powder by addition of diethyl ether to the dichloromethane solution.

IR spectroscopy has proved to be a valuable tool in assessing the degree of reduction and oligomerization of TCNE in its complexes. The IR spectrum of a Nujol mull of **3e** possessed intense absorptions at 2144 and 2183 cm^{-1} , indicating the presence of the $[\text{TCNE}]^-$ radical anion, and additional absorptions of comparable intensity at 1600 and 2197 cm^{-1} . These last two bands are not characteristic of TCNE,^{37–40} $[\text{TCNE}]^-$,^{35,39,41} $[\text{TCNE}]_2^{2-}$,⁴² or $[\text{TCNE}]^{2-43}$ or of the diamagnetic pentacyanopropenide³⁷ or tricyanoethenolate⁴⁴ ions, which are well-known decomposition products of $[\text{TCNE}]^-$.^{35,36,44–46}

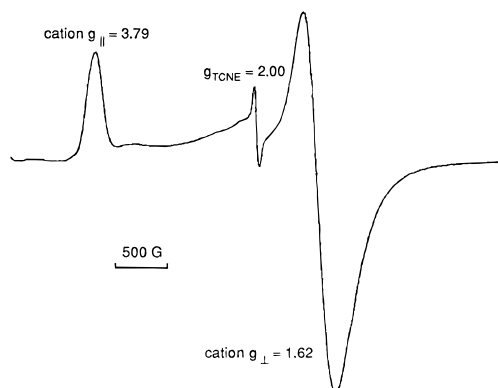


Figure 7. X-band ESR spectrum of **3e** in a dichloromethane glass at 13.5 K.

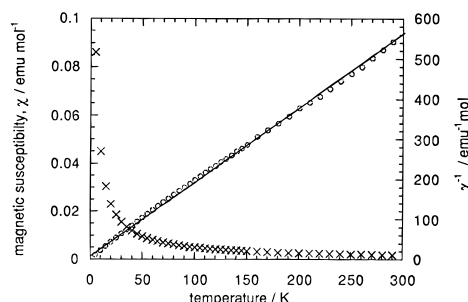


Figure 8. Magnetic susceptibility (χ , \times) and inverse magnetic susceptibility (χ^{-1} , \circ) per mole of Fe units, measured in a field of 0.1 T, for a sample of **3e**.

Room temperature ESR spectra of **3e**, either as a solid or as a dichloromethane solution, exhibit an isotropic absorption centered at $g = 2.00$; the solution spectra show hyperfine coupling characteristic of the TCNE^- radical anion. The spectrum of a dichloromethane glass at 13.5 K is shown in Figure 7 and shows, in addition to the $g = 2.00$ signal, an axially symmetrical pattern characteristic of a ferrocenium ion with $g_{\perp} = 1.62$ and $g_{\parallel} = 3.79$. The equations derived by Prins⁴⁷ show that Δg , defined as $g_{\parallel} - g_{\perp}$, is a useful probe of the distortion of a ferrocenium ion from D_5 symmetry. The degree of this distortion depends on the inherent symmetry of the cation but is also sensitive to the counterion and the medium in which the ESR spectrum is measured.^{47,48} In this case, the value of Δg , 2.17, is significantly lower than the values observed for ferrocenium (3.09)⁴⁷ and decamethylferrocenium (3.08, 3.11),⁴⁸ or even for the lower symmetry octamethylferrocenium ion (2.69).⁴⁹ However, similar values of Δg have been observed for other reduced symmetry species including 1,1'-dimethylferrocenium (2.16,⁴⁷ 2.08⁴⁸) and the $[\text{Fe}(\eta\text{-C}_5\text{H}_4)_2(\text{CH}_2)_3]^+$ ion (2.05, 2.19).⁴⁸ Solid-state magnetic susceptibility data were recorded for a sample of **3e** using a SQUID magnetometer and are shown in Figure 8; these indicated that the oxidized material obeys the Curie–Weiss law with $C = 0.549 \text{ emu mol}^{-1}$ of Fe and $\Theta = -1.1 \text{ K}$. The calculated effective moment (μ_{eff}) per mol of Fe is $2.0 \mu_{\text{B}}$. In the case of a fully oxidized material of the form $[\text{2e}]^{n+}[\text{TCNE}]^-_n$ one would expect a moment (using the average g value, $\langle g \rangle = 2.56$, determined by ESR) of $2.8 \mu_{\text{B}}$ (eq 1).

$$\mu_{\text{eff}}^2(\text{total for } [\text{2e}]^{n+}[\text{TCNE}]^-_n) = \frac{3}{4} \langle g_{\text{Fe}} \rangle^2 + 3 \quad (1)$$

If all the ferrocene units were oxidized and the salt contained only diamagnetic counterions, for example, $[\text{TCNE}]_2^{2-}$, one would still expect a moment of $2.2 \mu_{\text{B}}$. Therefore, the susceptibility data suggest that not all

the Fe centers have been oxidized. Microanalytical data are inconsistent with a simple formulation of the type $[2e]^{n+}[TCNE]_n^-$. The Weiss constant was calculated to be -1.1 K, indicating almost negligible long-range spin-spin exchange interactions.

We have also made preliminary investigations of the reactions of **2b** and **2d** with TCNE. Addition of 1 equiv of TCNE to **2d** in dichloromethane resulted in immediate darkening of the solution. Addition of petroleum ether results in precipitation of a dark brown solid, **3d**. Room temperature ESR spectra of dichloromethane solutions of this solid indicate the presence of a radical center with $g = 2.00$. Spectra at 25 K show, in addition to this $g = 2.00$ radical, an axially symmetrical pattern characteristic of a ferrocenium ion with $g_{\perp} = 1.51$, $g_{\parallel} = 4.05$, and $\Delta g = 2.54$. These data indicate a ferrocenium environment different from that in **3e**; this is consistent with the NMR and electrochemical data discussed above which indicate **2d** contains iron atoms in Cp^HFeCp^{Me} environments. Surprisingly, the IR spectrum of a film of the material does not show the $C\equiv N$ stretching frequencies characteristic of TCNE, $[TCNE]^-$, $[TCNE]_2^{2-}$, or $[TCNE]^{2-}$; a $C\equiv N$ band is observed at 2199 cm^{-1} , and a $C=C$ band at 1597 cm^{-1} implying the presence of a species similar to that present alongside $[TCNE]^-$ in **3e**. Together the ESR and IR data indicate at least some oxidation of the polymer and the formation of a paramagnetic cyano-carbon anion.

The addition of 1 equiv of TCNE to **2b** in dichloromethane resulted in a slight darkening of the solution. Precipitation with diethyl ether afforded a red-brown solid, **3b**. The room temperature ESR spectrum indicated that a radical species with $g = 2$ is present. An IR spectrum showed the presence of the same cyano-carbon species observed in **3d** and **3e**.

The presence of unusual cyano-carbon species in **3b**, **3d**, and **3e** is rather surprising, especially as we have found the poly(ferrocenylethylene) **2** ($M = Fe$, $ER_x = CH_2CH_2$) undergoes a much cleaner reaction with TCNE to yield reduced $[TCNE]_x^{y-}$ as the only cyano-carbon species in the product.⁵⁰ It is possible that this difference in behavior is related to the fact that the poly(ferrocenylsilanes) exhibit two oxidation waves, whereas the poly(ferrocenylethylenes) possess only very weak interaction between the iron centers;^{8,51} this may result in only half the ferrocene centers in a poly(ferrocenylsilane) undergoing initial electron transfer with TCNE. Further reaction between $[TCNE]^-$ and excess TCNE present may then account for the formation of the unusual cyano-carbon product and account for the elemental composition observed for **3e**.

It has often been found that the properties of salts of cyano anions such as TCNE are critically dependent on the methods of preparation and purification employed,^{42,46,49,52} so it may still be possible to synthesize magnetically interesting materials by variation of solvent, the ratio of reactants, the order of addition, and the electron-acceptor species.

Conclusions

Silicon-bridged [1]ferrocenophanes **1a–e** in which the Cp rings are substituted with up to eight methyl groups readily undergo TROP when heated in the melt to afford the corresponding methylated poly(ferrocenylsilanes). Increasing Cp methylation results in an increasing TROP onset temperature, as observed by DSC, but not in significant changes in ΔH_p . TROP of unsymmetrically methylated silicon-bridged [1]ferrocenophane **1d** affords poly(ferrocenylsilane) **2d** with three types of

silicon environments but only a single type of iron environment, consistent with TROP via nonselective cleavage of Si–Cp bonds. Cp methylation provides a method of manipulating the electronic properties of the poly(ferrocenylsilanes). The cyclic voltammetric half-wave oxidation potentials of the polymers are reduced by ca. 55 mV per Cp methyl substituent relative to the nonmethylated polymer **2a**, as expected based on small-molecule models, but the polymer UV–vis band II undergoes a red shift with increasing Cp methylation unlike small-molecule models. Cp methylation also affects poly(ferrocenylsilane) thermal behavior. The methylated poly(ferrocenylsilanes) are glassy and exhibit glass transitions which shift to higher temperature with increasing Cp methylation. Cp methylation leads to increased interchain distances consistent with increased steric bulk of the polymer backbone. Increasing Cp methylation leads to decreased polymer thermal stability with regard to weight loss.

In contrast to the results of Garnier and co-workers for oligo(ferrocenylsilanes),^{20d} we have found that unmethylated poly(ferrocenylsilanes) do not react with TCNE. However, the Cp methylated polymers readily react with TCNE, consistent with the effect of methylation upon their oxidation potentials. The products are more complex than the simple materials of the formula $[2]^{n+}[TCNE]_n^-$ one might anticipate. In the most fully investigated of these products, **3e**, magnetic susceptibility measurements show that not all the ferrocene moieties are oxidized and that the material obeys the Curie–Weiss law with no evidence of any magnetic ordering.

Experimental Section

Silicon-bridged [1]ferrocenophane monomers **1a–e**^{10,27} and poly(ferrocenylsilane) **2a**^{10,18} were prepared as previously described. Operations involving TCNE were carried out under nitrogen or in vacuo, using standard Schlenk procedures or a Vacuum Atmospheres glovebox and using solvents dried by distillation from P_2O_5 (dichloromethane) or sodium-potassium alloy (petroleum ether (bp 40–60 °C), diethyl ether). TCNE (Aldrich) was sublimed in vacuo prior to use. Solution NMR spectra were recorded on either Varian Gemini 200 or Varian XL 400 instruments. 1H NMR spectra were referenced to residual protonated C_6D_6 at 7.14 ppm, and ^{13}C spectra were referenced to the C_6D_6 signal at 128.0 ppm. ^{29}Si NMR spectra were recorded utilizing normal (proton coupled) pulse sequences. Solid-state ^{29}Si and ^{13}C NMR spectra were obtained using a Chemagnetics CMX 300 spectrometer equipped with a Chemagnetics magic angle spinning probe doubly tuned to the resonance frequencies of ^{29}Si (59.7 MHz) or ^{13}C (75.3 MHz). Samples were spun in a 7.5 mm o.d. zirconium rotor at a spinning rate of 6000 Hz. A single-contact cross-polarization technique was employed with a contact time of 5 ms and proton decoupling during the signal acquisition technique. The proton radiofrequency field strength was 50 kHz. Spectra were acquired using a sweep width of 50 kHz, a data size of 2 Hz, and a recycle delay of 5 s. All chemical shifts were referenced to external TMS. IR spectra were recorded on a Nicolet Magna 550 IR spectrometer or on a Mattson Instruments Polaris spectrometer. DSC analyses were performed at a heating/cooling rate of $10\text{ °C}\cdot\text{min}^{-1}$ under N_2 using a Perkin-Elmer DSC 7 differential scanning calorimeter. Since **1a–e** are moisture sensitive, samples for DSC analysis were hermetically sealed in aluminum pans under a N_2 atmosphere in a Vacuum Atmospheres glovebox and maintained under N_2 until analysis. Thermogravimetric analyses were performed at a heating rate of $10\text{ °C}\cdot\text{min}^{-1}$ under N_2 using a Perkin-Elmer TGA 7 thermogravimetric analyzer. Wide-angle X-ray scattering (WAXS) data were obtained at 25 °C using a Siemens D5000 diffractometer employing Ni-filtered $Cu\ K\alpha$ ($\lambda = 1.54178\text{ Å}$) radiation. Samples were scanned at step widths of 0.02° with 1.0 s per step in the Bragg angle range $3\text{--}40^\circ$.

Samples were prepared by spreading finely ground polymer on grooved plastic slides. Cyclic voltammograms were obtained under N_2 by analysis of methylene chloride solutions which were ca. 5×10^{-3} M in **2a–d** and 0.1 M in $[Bu_4N][PF_6]$ using an EG&G Princeton Applied Research Model 273 potentiostat/galvanostat. A Pt wire working electrode was used in conjunction with a W wire counter electrode and a Ag wire reference electrode in a Luggin capillary. Ferrocene was added as an internal standard, and all cyclic voltammograms are referenced to the ferrocene/ferrocenium ion couple at $E = 0.00$ V. UV–visible spectra were recorded on a Hewlett-Packard 8452A diode array spectrophotometer using a 1-cm quartz cell. Polymer ϵ values are quoted per repeat unit. Molecular weight estimates were made via gel permeation chromatography using a Waters Associates liquid chromatograph equipped with a 510 HPLC pump, U6K injector, Ultrastaygel gel columns with a pore size between 10^3 and 10^5 Å, and a Waters 410 differential refractometer. A flow rate of 1.0 mL/min was used and samples were dissolved in a THF solution of 0.1% tetra-*n*-butylammonium bromide. Polystyrene standards were used for calibration purposes. ESR measurements were performed in high-purity Spectrosil quartz tubes using an X-band Varian spectrometer; peaks were referenced by using a microcrystalline sample of 1,1-diphenyl-2-picrylhydrazyl (DPPH). Solid-state magnetic susceptibilities were measured on samples loaded in gelatin capsules using a Quantum Design MPMS-7 SQUID magnetometer. Data were corrected for the diamagnetism of the cores of the constituent atoms and for the diamagnetism of the sample holder, by extrapolation of χ vs $1/T$ to infinite temperature. Elemental analyses were performed by Quantitative Technologies Inc, Whitehouse, NJ, or by the Analytical Department of the Inorganic Chemistry Laboratory, Oxford.

Synthesis of $[Fe(\eta-C_5H_3Me)(\eta-C_5H_3Me)SiMe_2]_n$ (2b**): Cp–Me Groups at Random Positions.** A sample of 0.32 g of **1b** was flame-sealed in an evacuated (0.01 mmHg) Pyrex tube and heated at 150 °C for 3 h. The tube contents were dissolved in THF, filtered, and precipitated by addition to methanol. The fibrous orange solid was collected by filtration, reprecipitated (THF/methanol), collected by filtration, and dried in vacuo to afford 0.17 g (53%) of **2b** as a bright orange, fibrous solid: IR (thin film, KBr) 3070, 2961, 2919, 2888, 2868, 1396, 1245, 1155, 1096, 814, 797, 768 cm^{-1} ; 1H NMR (200 MHz, C_6D_6) δ 4.32–3.66 (6H, Cp–H), 1.93–1.78 (6H, Cp–CH₃), 0.78–0.49 (6H, Si–CH₃); ^{13}C NMR (100.6 MHz, C_6D_6) δ 88.4–86.4 (Cp–CH₃), 77.8–70.6 (Cp–H), 69.4–69.3 (Cp–Si), 16.0–13.7 (Cp–CH₃), 1.0 to –0.8 (Si–CH₃); ^{29}Si NMR (79.5 MHz, C_6D_6) δ –6.2 to –6.7; GPC $M_w = 4.1 \times 10^5$, $M_n = 2.8 \times 10^5$, PDI (M_w/M_n) = 1.5. Anal. Calcd for $C_{14}H_{18}FeSi$: C, 62.23; H, 6.71. Found: C, 61.91; H, 7.02.

Synthesis of $[Fe(\eta-C_5H_3Me)(\eta-C_5H_3Me)SiMe_2]_n$ (2c**): Cp–Me Groups at the 3,3' Positions.** A sample of 0.21 g of **1c** was flame-sealed in an evacuated (0.01 mm Hg) Pyrex tube and heated at 150 °C for 3 h. The tube contents were dissolved in THF, filtered, and precipitated by addition to methanol. The fibrous orange solid was collected by filtration, reprecipitated (THF/hexanes), collected by filtration, and dried in vacuo to afford 0.19 g (91%) of **2c** as a bright orange, fibrous solid: IR (thin film, KBr) 3069, 2961, 2920, 2867, 1395, 1246, 1155, 1096, 1038, 797, 769 cm^{-1} ; 1H NMR (200 MHz, C_6D_6) δ 4.03 (s, 2H, Cp–H), 3.96–3.95 (m, 2H, Cp–H), 3.86 (s, 2H, Cp–H), 2.00–1.99 (m, 6H, Cp–CH₃), 0.63 (s, 6H, Si–CH₃); ^{13}C NMR (100.6 MHz, C_6D_6) δ 88.3–86.4 (Cp–CH₃), 77.6–69.3 (Cp–H, Cp–Si), 15.7–13.8 (Cp–CH₃), 0.66 to –0.49 (Si–CH₃); ^{29}Si NMR (79.5 MHz, C_6D_6) δ –6.3, –6.5; GPC $M_w = 1.8 \times 10^5$, $M_n = 9.4 \times 10^4$, PDI (M_w/M_n) = 1.9. Anal. Calcd for $C_{14}H_{18}FeSi$: C, 62.23; H, 6.71. Found: C, 62.62; H, 7.02.

Synthesis of $[Fe(\eta-C_5Me_4)(\eta-C_5H_4)SiMe_2]_n$ (2d**).** A sample of 0.27 g (0.91 mmol) of **1d** was flame-sealed in an evacuated (0.01 mmHg) Pyrex tube and heated at 150 °C for 1 h. The contents were dissolved in THF, filtered, and precipitated by addition to methanol. The fibrous orange solid was collected by filtration, washed with additional methanol, and dried in vacuo to afford 0.17 g (63%) of **2d** as a fibrous, orange solid: IR (KBr, thin film) 3082, 2964, 2906, 2863, 1381, 1330, 1244, 1161, 1071, 1034, 816, 799, 766 cm^{-1} ; 1H NMR (200.0 MHz, C_6D_6) δ 4.04–3.82 (br m, 4H, Cp–H), 1.95–1.79 (br m, 12H,

Cp–CH₃), 0.99–0.96 (br m), 0.82 (br s), 0.64 (br s) (6H, 1:2:1 ratio, Si–CH₃); ^{13}C NMR (100.6 MHz, C_6D_6) δ 85.7, 85.4, 84.8–84.6 (Cp–Me), 76.1, 76.0, 75.4–74.5 (Cp–H), 68.3–67.9 (Cp–Si), 14.9, 14.8, 12.4, 12.3 (Cp–CH₃), 5.1, 1.5, –0.22 to –0.26 (Si–CH₃); ^{29}Si NMR (79.4 MHz, C_6D_6) δ –4.03 to –4.07, –6.36 to –6.48, –6.76 to –6.78; GPC $M_w = 3.4 \times 10^5$, $M_n = 2.3 \times 10^5$, PDI (M_w/M_n) = 1.43. Anal. Calcd for $C_{16}H_{22}FeSi$: C, 64.43; H, 7.43. Found: C, 64.69; H, 7.79.

Synthesis of $[Fe(\eta-C_5Me_4)(\eta-C_5Me_4)SiMe_2]_n$ (2e**).** A sample of 0.20 g of **1e** was flame-sealed in an evacuated (0.01 mmHg) Pyrex tube and heated at 255 °C for 9 h. The tube contents were extracted with THF for 48 h and then dried in vacuo to afford 0.12 g (60%) of **2e** as a bright orange, powdery solid: IR (KBr) 2963, 2900, 2859, 1669, 1472, 1454, 1378, 1249, 1118, 1029, 840, 811, 764 cm^{-1} ; ^{13}C NMR (CPMAS) δ 85–82 (Cp–CH₃), 69 (Cp–Si), 18–4 (Cp–CH₃, Si–CH₃); ^{29}Si NMR (CPMAS) δ –1.6. Anal. Calcd for $C_{20}H_{30}FeSi$: C, 67.78; H, 8.53. Found: C, 67.50; H, 8.46.

Reactions of Polymers **2a**, **2b**, **2d**, and **2e** with TCNE.

Reaction of **2a with TCNE.** A solution of 34 mg (0.27 mmol) of TCNE in 20 mL of dichloromethane was added dropwise to a stirred solution of 59 mg (0.24 mmol of monomer units) of **2a** in 20 mL of dichloromethane. After 18 h, no visible reaction had occurred. The solvent was removed in vacuo to afford orange solids which were analyzed by infrared spectroscopy. Selected IR data (thin film, KBr): 2219, 2255 cm^{-1} .

The reactions of the model compound $(Fe(\eta-C_5H_4)SiMe_2Fc)_2$ ($Fc = Fe(\eta-C_5H_4)(\eta-C_5H_5)$) and **2** ($M = Fe$, $ER_x = SiBu_2$) with TCNE were carried out in an analogous fashion and resulted in identical $C \equiv N$ IR bands.

Reaction of **2b with TCNE: Synthesis of **3b**.** A solution of 50 mg (0.39 mmol) of TCNE in 20 mL of dichloromethane was added dropwise to a solution of 100 mg (0.37 mmol of monomer units) of **2b** in 20 mL of dichloromethane; the reaction mixture slowly darkened. After 18 h the solvent volume was reduced in vacuo to 20 mL, and 130 mL of diethyl ether was added. The resulting reddish precipitate was washed with 2×50 mL of diethyl ether and dried in vacuo. Selected IR data (thin film, KBr): 1597, 2199 cm^{-1} . ESR (CH_2Cl_2 solution, room temperature): $g = 2.00$.

Reaction of **2d with TCNE: Synthesis of **3d**.** A solution of 43 mg (0.34 mmol) of TCNE in 10 mL of dichloromethane was added dropwise to a solution of 97 mg (0.33 mmol of monomer units) of **2d** in 20 mL of dichloromethane; the reaction mixture instantly darkened. After 18 h, the reaction mixture was filtered before solvent removal in vacuo. The solids were washed with 2×100 mL of diethyl ether, redissolved in dichloromethane, and precipitated by addition of petroleum ether (bp 40–60 °C). Selected IR data (thin film, KBr): 1597, 2199 cm^{-1} . ESR (CH_2Cl_2 glass, 25 K): cation $g_{||} = 4.05$, $g_{\perp} = 1.51$, $\langle g \rangle = 2.69$; anion $g = 2.00$.

Reaction of **2e with TCNE: Synthesis of **3e**.** A solution of 40 mg (0.31 mmol) of TCNE in 10 mL of dichloromethane was added dropwise to a suspension of 100 mg (0.28 mmol of monomer units) of **2e** in 5 mL of dichloromethane; the reaction mixture instantly darkened, and the polymer slowly dissolved. Addition of more dichloromethane resulted in almost complete dissolution; this green-red dichroic solution was filtered, leaving a small quantity of a dark solid (selected IR data: 1602, 2204 cm^{-1}). After the solution volume was reduced in vacuo to 30 mL, 150 mL of diethyl ether was added. The supernatant was filtered from the resulting green solids, **3b**, which were washed with 100 mL of diethyl ether before drying in vacuo. Selected IR data (Nujol, KBr): 1600, 2144, 2183, 2197 cm^{-1} . ESR (CH_2Cl_2 glass, 13.5 K): cation $g_{||} = 3.79$, $g_{\perp} = 1.62$, $\langle g \rangle = 2.56$; TCNE- $g = 2.00$. Magnetic susceptibility (per Fe): $\mu_{eff} = 2.0 \mu_B$, $\Theta = -1.1$ K. Anal. Calcd for $[2e]^{+}[TCNE]^{-}$, $C_{26}H_{30}FeN_4Si$: C, 64.72; H, 6.27; N, 11.61; Fe, 11.57. Found: C, 61.54; H, 6.84; N, 6.29; Fe, 11.66. The low N analysis suggests that CN loss may accompany the formation of the polyanion present.

Acknowledgment. I.M. thanks the Natural Sciences and Engineering Research Council of Canada (NSERC), the Institute for Chemical Science and Technology (ICST), and the Petroleum Research Fund (PRF)

administered by the American Chemical Society, for funding and the Alfred P. Sloan Foundation for a Research Fellowship (1994–1996). D. O'H. would like to acknowledge EPSRC for financial support and a studentship (S.B.). The authors also thank Prof. R. H. Morris for the use of the electrochemical equipment.

References and Notes

- Miller, J. S.; Epstein, A. J.; Reiff, W. M. *Acc. Chem. Res.* **1988**, *21*, 114–120.
- Miller, J. S.; Epstein, A. J.; Reiff, W. M. *Chem. Rev.* **1988**, *88*, 201–220.
- O'Hare, D. *Chem. Soc. Rev.* **1992**, 121–126.
- Atzkern, H.; Bergerat, P.; Fritz, M.; Hiermeier, J.; Hudeczek, P.; Kahn, O.; Kanellakopulos, B.; Köhler, F. H.; Ruhs, M. *Chem. Ber.* **1994**, *127*, 277–286.
- Hughes, A. K.; Murphy, V. J.; O'Hare, D. *J. Chem. Soc., Chem. Commun.* **1994**, 163–164.
- (a) Nugent, H. M.; Rosenblum, M.; Klemarczyk, P. *J. Am. Chem. Soc.* **1993**, *115*, 3848. (b) Brandt, P. F.; Rauchfuss, T. B. *J. Am. Chem. Soc.* **1992**, *114*, 1926. (c) Bayer, R.; Pöhlmann, T.; Nuyken, O. *Makromol. Chem., Rapid Commun.* **1993**, *14*, 359. (d) Wright, M. E.; Toplikar, E. G. *Contemp. Top. Polym. Sci.* **1992**, *7*, 285–292.
- For reviews of metal-based polymers, see: (a) Pittman, C. U., Jr.; Carraher, C. E., Jr.; Reynolds, J. R. In *Encyclopedia of Polymer Science and Engineering*; Mark, H. F., Bikales, N. M., Overberger, C. G., Menges, G., Eds.; Wiley: New York, 1989; Vol. 10, p 541. (b) Sheats, J. E.; Carraher, C. E., Jr.; Pittman, C. U., Jr.; Zeldin, M.; Currell, B. *Inorganic and Metal-Containing Polymeric Materials*; Plenum: New York, 1989. (c) Gonsalves, K. E.; Rausch, M. D. In *Inorganic and Organometallic Polymers*; Zeldin, M., Wynne, K. J., Allcock, H. R., Eds.; ACS Symposium Series 360; American Chemical Society: Washington, DC, 1988; Chapter 36.
- Manners, I. *Adv. Organomet. Chem.* **1995**, *37*, 131 and references cited therein.
- Mueller-Westerhoff, U. T.; Nazzari, A.; Tanner, M. *J. Organomet. Chem.* **1982**, *236*, C41.
- Foucher, D. A.; Tang, B.-Z.; Manners, I. *J. Am. Chem. Soc.* **1992**, *114*, 6246–6248.
- Rosenberg, H. U.S. Patent 3,426,053, 1969.
- Rulkens, R.; Lough, A. J.; Manners, I. *J. Am. Chem. Soc.* **1994**, *116*, 797–798.
- Rulkens, R.; Ni, Y.; Manners, I. *J. Am. Chem. Soc.* **1994**, *116*, 12121.
- Ni, Y.; Rulkens, R.; Pudelski, J. K.; Manners, I. *Makromol. Chem., Rapid Commun.* **1995**, *16*, 637.
- (a) Foucher, D. A.; Manners, I. *Makromol. Chem., Rapid Commun.* **1993**, *14*, 63–66. (b) Foucher, D. A.; Edwards, M.; Burrow, R. A.; Lough, A. J.; Manners, I. *Organometallics* **1994**, *13*, 4959–4966. (c) Manners, I. In *Inorganic and Organometallic Polymers: II*; Wisian-Neilson, P., Allcock, H. R., Wynne, K., Eds.; ACS Symposium Series 572; Washington, DC, 1994; p 449.
- Nelson, J. M.; Rengel, H.; Manners, I. *J. Am. Chem. Soc.* **1993**, *115*, 7035–7036.
- Nelson, J. M.; Lough, A. J.; Manners, I. *Angew. Chem., Int. Ed. Engl.* **1994**, *33*, 989–991.
- Foucher, D. A.; Ziembinski, R.; Tang, B.-Z.; Macdonald, P. M.; Massey, J.; Jaeger, C. R.; Vancso, G. J.; Manners, I. *Macromolecules* **1993**, *26*, 2878–2884.
- (a) Foucher, D.; Ziembinski, R.; Petersen, R.; Pudelski, J.; Edwards, M.; Ni, Y.; Massey, J.; Jaeger, C. R.; Vancso, G. J.; Manners, I. *Macromolecules* **1994**, *27*, 3992–3999. (b) Pudelski, J. K.; Rulkens, R.; Foucher, D. A.; Lough, A. J.; Macdonald, P. M.; Manners, I. *Macromolecules* **1995**, *28*, 7301–7308.
- For the work of other groups on poly(ferrocenylsilanes) and related materials, see: (a) Reference 8. (b) Tanaka, M.; Hayashi, T. *Bull. Chem. Soc. Jpn.* **1993**, *66*, 334. (c) Nguyen, M. T.; Diaz, A. F.; Dement'ev, V. V.; Pannell, K. H. *Chem. Mater.* **1993**, *5*, 1389. (d) Hmyene, M.; Yasser, A.; Escorne, M.; Percheron-Guegan, A.; Garnier, F. *Adv. Mater.* **1994**, *6*, 564.
- Miller, J. S.; Glatzhofer, D. T.; O'Hare, D. M.; Reiff, W. M.; Chakraborty, A.; Epstein, A. J. *Inorg. Chem.* **1989**, *28*, 2930–2939.
- Gassman, P. G.; Macomber, D. W.; Hershberger, J. W. *Organometallics* **1983**, *2*, 1470–1472.
- Gassman, P. G.; Winter, C. H. *J. Am. Chem. Soc.* **1988**, *110*, 6130–6135.
- Gassman, P. G.; Winter, C. H. *Organometallics* **1991**, *10*, 1592–1598.
- Gassman, P. G.; Mickelson, J. W.; Sowa, J. R. *J. Am. Chem. Soc.* **1992**, *114*, 6942–6944.
- See, for example: (a) Miller, J. S.; Epstein, A. J. *Angew. Chem., Int. Ed. Engl.* **1994**, *33*, 384–415. (b) Miller, J. S.; Calabrese, J. C.; Rommelmann, H.; Chittipeddi, S.; Zhang, J. H.; Reiff, W. M.; Epstein, A. J. *J. Am. Chem. Soc.* **1987**, *109*, 769. (c) Broderick, W. E.; Hoffman, B. M. *J. Am. Chem. Soc.* **1991**, *113*, 6334. (d) Yee, G. T.; Manriquez, J. M.; Dixon, D. A.; Mclean, R. S.; Groski, D. M.; Flippen, R. B.; Narayan, K. S.; Epstein, A. J.; Miller, J. S. *Adv. Mater.* **1991**, *3*, 309–311.
- Pudelski, J. K.; Foucher, D. A.; Honeyman, C. H.; Lough, A. J.; Manners, I.; Barlow, S.; O'Hare, D. *Organometallics* **1995**, *14*, 2470–2479.
- Pudelski, J. K.; Manners, I. *J. Am. Chem. Soc.* **1995**, *117*, 7265.
- Elschenbroich, C.; Salzer, A. *Organometallics: A Concise Introduction*; VCH: Weinheim, 1992.
- Hultsch, K.; Nelson, J. M.; Lough, A. J.; Manners, I. *Organometallics* **1995**, *14*, 5496–5502.
- Osborne, A. G.; Whiteley, R. H.; Meads, R. E. *J. Organomet. Chem.* **1980**, *193*, 345.
- Sohn, Y. S.; Hendrickson, D. N.; Gray, H. B. *J. Am. Chem. Soc.* **1971**, *93*, 3603.
- Rasburn, J.; Petersen, R.; Rulkens, R.; Manners, I.; Vancso, G. J. *Chem. Mater.* **1995**, *7*, 871.
- (a) Tang, B.-Z.; Petersen, R.; Foucher, D. A.; Lough, A. J.; Coombs, N.; Sodhi, R.; Manners, I. *J. Chem. Soc., Chem. Commun.* **1993**, 523–525. (b) Petersen, R.; Foucher, D. A.; Tang, B.-Z.; Lough, A. J.; Raju, N. P.; Greedan, J. E.; Manners, I. *Chem. Mater.* **1995**, *7*, 2045–2053.
- Webster, O. W.; Mahler, W.; Benson, R. E. *J. Am. Chem. Soc.* **1962**, *84*, 3678–3684.
- Rosenblum, M.; Fish, R. W.; Bennett, C. *J. Am. Chem. Soc.* **1964**, *86*, 5166–5170.
- Looney, C. E.; Downing, J. R. *J. Am. Chem. Soc.* **1958**, *80*, 2840–2844.
- Miller, F. A.; Sala, O.; Devlin, P.; Overend, J.; Lippert, E.; Lunder, W.; Moser, H.; Varchim, J. *Spectrochim. Acta* **1964**, *1233*–1247.
- Stanley, J.; Smith, D.; Latimer, B.; Devlin, J. P. *J. Phys. Chem.* **1966**, *70*, 2011–2016.
- Hinkel, J. J.; Devlin, J. P. *J. Chem. Phys.* **1973**, *58*, 4750–4756.
- Rettig, M. F.; Wing, R. M. *Inorg. Chem.* **1969**, *8*, 2685–2689.
- Miller, J. S.; O'Hare, D. M.; Chakraborty, A.; Epstein, A. J. *J. Am. Chem. Soc.* **1989**, *111*, 7853–7859.
- Dixon, D. A.; Miller, J. S. *J. Am. Chem. Soc.* **1987**, *109*, 3656–3664.
- Sullivan, B. W.; Foxman, B. M. *Organometallics* **1983**, *2*, 187–189.
- Middleton, W. J.; Little, E. L.; Coffman, D. D.; Englehardt, V. A. *J. Am. Chem. Soc.* **1958**, *80*, 2795–2806.
- Miller, J. S.; Calabrese, J. C.; Rommelmann, H.; Chittipeddi, S. R.; Zhang, J. H.; Reiff, W. M.; Epstein, A. J. *J. Am. Chem. Soc.* **1987**, *109*, 769–781.
- Prins, R. *Mol. Phys.* **1970**, *19*, 603–620.
- Duggan, D. M.; Hendrickson, D. N. *Inorg. Chem.* **1975**, *14*, 955–969.
- Miller, J. S.; Glatzhofer, D. T.; O'Hare, D. M.; Reiff, W. M.; Chakraborty, A.; Epstein, A. J. *Inorg. Chem.* **1989**, *28*, 2930–2939.
- Nelson, J.; Rengel, H.; Lough, A. J.; Manners, I.; Barlow, S.; O'Hare, D., unpublished results.
- Foucher, D. A.; Honeyman, C. H.; Nelson, J. M.; Tang, B.-Z.; Manners, I. *Angew. Chem., Int. Ed. Engl.* **1993**, *32*, 1709–1711.
- Miller, J. S.; Zhang, J. H.; Reiff, W. M.; Dixon, D. A.; Preston, L. D.; Reis, A. H., Jr.; Gebert, E.; Extine, M.; Troup, J.; Epstein, A. J.; Ward, M. D. *J. Chem. Phys.* **1987**, *91*, 4344–4360.